

Coordination of Growth and Cell Division in the *Drosophila* Wing

Thomas P. Neufeld, Aida Flor A. de la Cruz,
Laura A. Johnston, and Bruce A. Edgar*
Division of Basic Sciences
Fred Hutchinson Cancer Research Center
1100 Fairview Avenue North
Seattle, Washington 98109

Summary

In most tissues, cell division is coordinated with increases in mass (i.e., growth). To understand this coordination, we altered rates of division in cell clones or compartments of the *Drosophila* wing and measured the effects on growth. Constitutive overproduction of the transcriptional regulator dE2F increased expression of the S- and M-phase initiators Cyclin E and String (Cdc25), thereby accelerating cell proliferation. Loss of dE2F or overproduction of its corepressor, RBF, retarded cell proliferation. These manipulations altered cell numbers over a 4- to 5-fold range but had little effect on clone or compartment sizes. Instead, changes in cell division rates were offset by changes in cell size. We infer that dE2F and RBF function specifically in cell cycle control, and that cell cycle acceleration is insufficient to stimulate growth. Variations in dE2F activity could be used to coordinate cell division with growth.

Introduction

Most cells double their mass during each division cycle, maintaining a roughly constant size as they proliferate (Mitchison, 1971). Yet, it remains unclear how the biosynthesis that constitutes growth is coordinated with cell cycle controls. A paradigm for approaching this problem arose from studies pioneered in yeast by Hartwell (1971) and Nurse et al. (1976), who identified cell proliferation mutants of two general classes. One type of mutant blocked cell cycle progression while allowing cell growth to continue, and the other arrested cell growth and division coordinately. Mutations in this first class are now known to affect cell cycle control, whereas those in the second class generally affect biosynthesis. The distinct phenotypes of these mutants highlight the fact that in yeast, cell cycle progression and cell growth are separable processes which are normally coupled, and that growth is dominant and rate-limiting (Johnston et al., 1977).

Despite its simplicity, confirmation of this paradigm has been slow in higher eukaryotes. There are examples in metazoans of specific cell cycle alterations that uncouple growth from division, resulting in altered cell size (Franch et al., 1995; Hemerly et al., 1995; Sheikh et al., 1995; Fero et al., 1996; Kipreos et al., 1996; Weigmann et al., 1997). This suggests that the dominance of growth over cell cycle controls is conserved. However, several

vertebrate regulators that are thought to function specifically in cell cycle control have also been implicated in growth control (Sherr, 1996). An interesting case is the *retinoblastoma* tumor suppressor (pRB), which is believed to function as a cell cycle inhibitor. Recent studies show that pRB can throttle RNA pol I and pol III transcription (Cavanaugh et al., 1995; White et al., 1996) and that cells lacking pRB will proliferate at doses of cycloheximide which arrest control cells (Herrera et al., 1996). This suggests that pRB might directly suppress growth by reducing a cell's protein synthetic capacity and thus affect cell cycle progression only indirectly. If this were true the various factors that interact with pRB—Cyclins D and E, CDKs 2, 4, and 6, the E2F transcription factors, and the CDK inhibitor p16—would also be expected to affect general biosynthesis. This might explain why mutations in these genes are so frequently associated with cellular transformation and carcinogenesis. Alternatively, these molecules might be integral parts of a mechanism that senses growth and regulates the activity of cell cycle control genes accordingly (Rosenwald et al., 1995; Aktas et al., 1997; Leone et al., 1997; Peeper et al., 1997). Studies in cell culture seem to support this latter possibility (Ohtsubo and Roberts, 1993; Quelle et al., 1993; Reznitsky et al., 1994; Franch et al., 1995), but since the effects of these regulators on increases in mass are rarely measured, this issue remains unresolved.

Here, we address these issues in the developing wing of *Drosophila melanogaster*. The wing originates from an embryonic primordium of about 50 cells, which are organized into an epithelial "disc." These cells proliferate exponentially in the larva, roughly double their mass during each 10–12 hr cycle, and reach about 50,000 in number before they differentiate (Garcia-Bellido and Merriam, 1971; Madhavan and Schneiderman, 1977). As in vertebrate development, cell proliferation in the wing is directed by region-specific, secreted signals that act through the WG/WNT, DPP/BMP, VN/EGF, Notch, and Hedgehog pathways (Zecca et al., 1995; Burke and Basler, 1996; Doherty et al., 1996; Lecuit et al., 1996; Schnepf et al., 1996; Karim and Rubin, 1998; see Serrano and O'Farrell, 1997, for review). Paradoxically, although wing growth is driven by spatially patterned signals, cell proliferation occurs ubiquitously during the growth phase, with little obvious patterning (Garcia-Bellido and Merriam, 1971; González-Gaitán et al., 1994; Milán et al., 1996a, 1996b). The lack of concordance between signaling and proliferation patterns suggests that their connection is probably indirect. Perhaps cell signaling modulates growth, and growth rates are monitored by an intermediary mechanism that regulates the activity of cell cycle control genes to match (Bryant, 1996; Edgar and Lehner, 1996).

As noted above, two candidate players in this growth monitoring mechanism are the dE2F transcription factor and its corepressor RBF, a fly homolog of pRB (Dylnacht et al., 1994; Ohtani and Nevins, 1994; Du et al., 1996b). E2F activates genes required for S phase in both *Drosophila* and vertebrates and promotes cell cycle progression in diverse cell types (Johnson et al., 1993;

*To whom correspondence should be addressed.

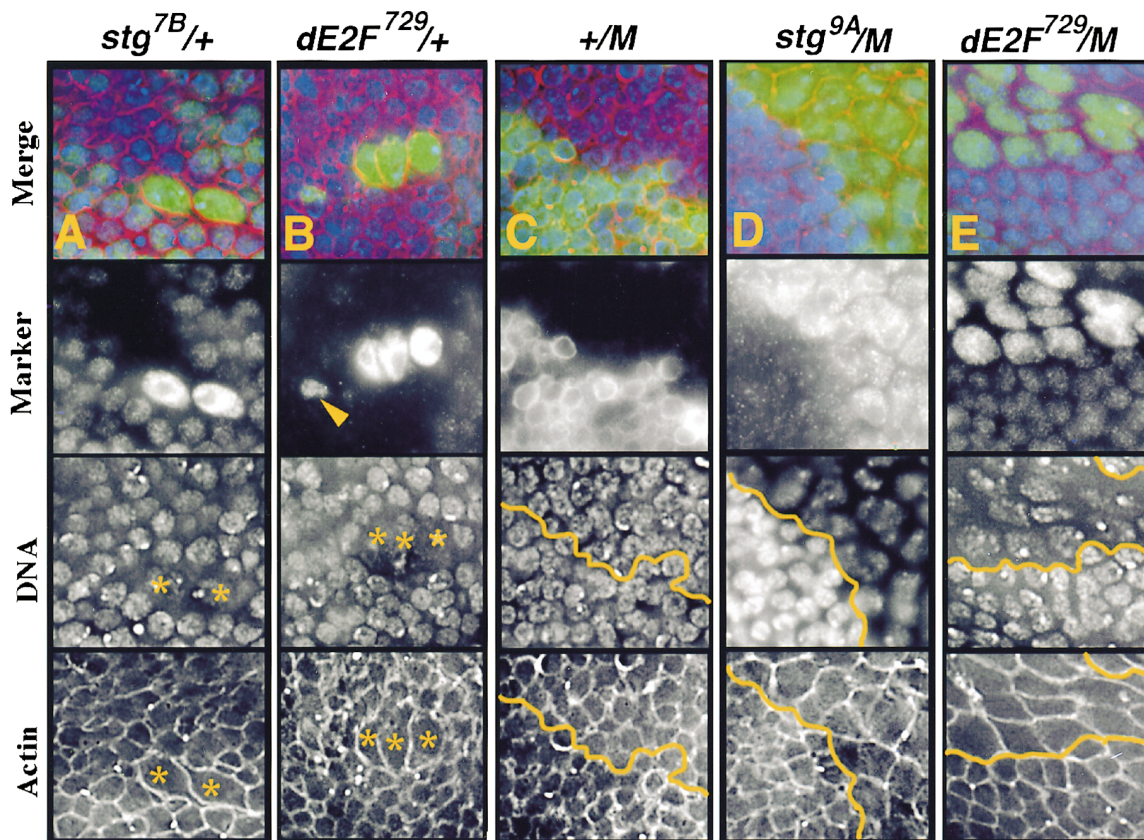


Figure 1. Enlargement and Death of *stg* and *dE2F* Mutant Cells

(A) 48-hr-old *stg*^{7B} cells in the wing pouch induced by FLP/FRT-mediated somatic recombination. Cells are stained for the clonal marker (π -myc; green), DNA (blue), and Actin (red). The enlarged mutant cells are positively stained with the two copies of the π -myc and marked with yellow asterisks in the lower two panels. *+/+* twinstots lacking π -myc are larger than the area photographed. Genotype, *hs-FLP; FRT(82B) stg*^{7B} π -myc/*FRT(82B)*.

(B) 48-hr-old *E2F*⁷²⁹ cells in the wing pouch positively marked with two copies of LacZ and denoted by yellow asterisks. Three mutant cells are enlarged, and the fourth is apoptotic (arrowhead). Genotype, *hs-FLP; FRT(82B) E2F*⁷²⁹ LacZ/*FRT(82B)*.

(C) A mosaic of *Minute*⁺ and *Minute* cells, showing that *Minute* cells (dark) are normal in size. The *Minute* mutation is a recessive cell lethal, so no twin spot is seen. Genotype, *hs-FLP; FRT(82B) N-myc/FRT(82B) M(3)95A*.

(D) A mosaic of *stg*^{9A}/*stg*^{9A} *M*⁺ and *stg*^{9A}/*+* *M* cells at semipermissive temperature. The *stg*^{9A}/*stg*^{9A} mutant cells are positively marked with two copies of π -myc and are grossly enlarged. Genotype, *hs-FLP; FRT(82B) stg*^{9A} π -myc/*FRT(82B) M(3)95A*.

(E) Enlarged *E2F*⁷²⁹ cells in a *Minute* background. Genotype, *hs-FLP; FRT(82B) E2F*⁷²⁹ LacZ/*FRT(82B) M(3)95A*.

Asano et al, 1996; Duronio et al., 1996; Rozman et al., 1997). RBF counteracts these effects (Du et al, 1996a). Previous studies suggested that the critical proximal regulators of the wing disc cell cycle are Cyclin E (CYCE), which promotes S phase initiation, and String (STG), a Cdc25-type phosphatase that promotes mitosis (Milán et al., 1996a, 1996b). Here, we use the FLP/FRT and GAL4/UAS techniques to delete or overproduce these four genes in the growing wing. We show that they are rate-limiters of the disc cell cycle and that *dE2F* can modulate rates of cell proliferation by regulating transcription of both *cyclin E* and *string*. Although slowing the cell cycle suppresses growth, we find that accelerating the cell cycle is insufficient to stimulate growth.

Results

Cell Cycle Arrest Allows Continued Growth but Leads to Cell Death

To determine the effect of cell cycle arrest on disc cell growth, we used mitotic recombination to delete cell

cycle gene functions (Xu and Rubin, 1993). This confirmed that *string*, *cyclin E*, and *dE2F* are each required for imaginal cell proliferation and revealed a common fate for disc cells that sustain a cell cycle arrest or delay. Cells homozygous for a null allele of *string* (*stg*^{7B}) divided only once, implying that *string* must be transcribed at least every two cell cycles. Arrested *stg*^{7B} cells became enlarged, indicating that cell growth continued after the arrest (Figure 1A). Arrested cells were gradually lost from the disc epithelium (Table 1) through a process termed "cell competition" (Simpson, 1979). Slowly dividing cells, generated using a temperature-sensitive *string* allele (*stg*^{9A}), also enlarged and were also eliminated, though more slowly than the nondividing *stg*^{7B} cells (Table 1). Cells homozygous for a null *dE2F* allele (*dE2F*⁷²⁹) achieved clone sizes of up to 15 cells but otherwise behaved much like *string* mutant cells: they enlarged and were then lost (Figure 1B and Table 1; Brook et al., 1996). The largest *dE2F*⁷²⁹ cells were observed basal to the disc epithelium, a location shared with apoptotic *dE2F*⁷²⁹ cells (Figure 1B), and apoptotic cells induced by other treat-

Table 1. Elimination of Arrested or Slowly Dividing Mutant Cells; Percent Surviving Mutant Clones

	<i>dE2F⁷²⁹</i>	<i>stg^{7B}</i>	<i>stg^{9A}</i>	<i>stg^{9A}</i>	<i>stg^{9A}</i>
PHS (hr)	(null) % (N)	(null) % (N)	(ts; 30°) % (N)	(ts; 23°) % (N)	(ts; 18°) % (N)
24 hr	94 (52)	74 (39)	34 (115)	56 (126)	81 (81)
48 hr	62 (83)	6 (33)	4 (106)	15 (109)	75 (93)
72 hr	5 (38)	0 (15)	1 (73)	2 (88)	36 (104)

The gradual elimination of *E2F⁷²⁹*, *stg^{7B}*, and temperature-sensitive *stg^{9A}* cells at various temperatures. The frequencies of *+/+* clones (twinspots) with and without associated mutant cell clones were tallied. Values displayed are percentages representing the frequencies of surviving mutant clones 24, 48, or 72 hr after clone induction (Number of mutant clones paired with *+/+* clones/Total *+/+* clones × 100). (N) represents number of clones scored.

ments (Figure 4E). These observations suggest a progression in which cells experiencing cell cycle arrest continue to grow, are displaced from the disc epithelium, and finally undergo apoptosis. This fate may be common to all cells that sustain an inappropriate cell cycle arrest in the disc, since cells homozygous for null alleles of *cdc2* (*B47*) or *cyclin E* (*AR95*) also produced clones of 2–4 cells, which enlarged and then died (data not shown). Although cell growth continued after cell cycle arrest, clones of arrested cells produced far less tissue mass than their wild-type sister clones (twinspots). This is probably due to a size limit imposed by DNA content, since nondividing disc cells that are capable of continued DNA endoreplication can grow to much larger sizes than these (Weigmann et al., 1997).

In further tests we used a *Minute* mutation, *M(3)95A*, to confer a relative growth advantage upon cells homozygous for *stg^{9A}* or *dE2F⁷²⁹*. Like most *Minutes* so far cloned, *M(3)95A* is a loss-of-function mutation in a ribosomal protein (rpS3; Andersson et al., 1994). It is lethal to disc cells when homozygous, but it slows their growth when heterozygous. In mosaic discs wild-type cells (*Minute⁻* or *M⁺*) out-compete the more slowly growing *Minute* (*M*) cells and produce abnormally large clones that can encompass up to half the disc (García-Bellido et al., 1973; Simpson, 1979; Simpson and Morata, 1981). Despite these effects on clonal growth, we found that *M(3)95A* did not alter cell size (Figure 1C, FACS data not shown). Hence, when cell growth is slowed in the wing, cell cycle progression evidently slows in a coordinate fashion.

Although *stg^{9A}* *M⁺* cells in an *M* background did not survive at temperatures that blocked cell division completely (≥29°C), at semipermissive temperatures they produced clones of >100 cells (Figure 1D). The degree of cell enlargement in these clones was inversely correlated with division rate: at 23°C *stg^{9A}* *M⁺* cells were grossly enlarged, but at 18°C they showed only modest increases in cell size. We obtained similar results when *M(3)95A* was used to confer a relative growth advantage upon *dE2F⁷²⁹* mutant cells. In an *M* background, *dE2F⁷²⁹* *M⁺* cells achieved clone sizes of up to 50 cells and showed vastly increased cell size (Figure 1E). The enlargement of *dE2F* mutant cells suggests that like *string*, *dE2F* primarily regulates cell cycle progression, not cell growth. The observation that *dE2F*-null cells produced large clones in a *Minute* background indicates that *dE2F*

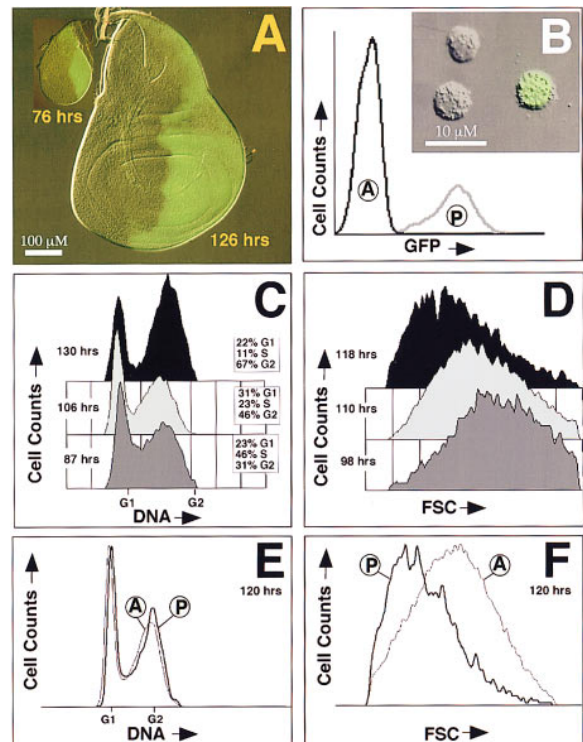


Figure 2. Disc Cell Sizes Change According to Stage and Identity (A) en-GAL4, UAS-GFP wing discs at 76 hr and 126 hr AED, showing posterior compartment expression of GFP, and the overall growth during this period. Posterior is to the right in all figures. (B) Plot of GFP intensity, showing separation of anterior (A) and posterior (P) cells. The inset shows two GFP⁻ cells and one GFP⁺ cell from a dissociated disc, photographed using DIC and fluorescence. (C) DNA content of total wing disc cells measured by FACS at 87 hr, 106 hr, and 130 hr AED. During this interval the S phase fraction shrinks and cells accumulate in G2. (D) Disc cell size, as measured by forward scatter (FSC), decreases between 98 and 118 hr AED. (E) At 120 hr AED anterior (A) and posterior (P) cells have similar G1/S/G2 phasing. (F) FSC of the same 120 hr cell sample as in (E), showing that P cells are smaller than A cells at this time point.

is not absolutely required for cell cycle progression but merely accelerates it (see also Brook et al., 1996; Royzman et al., 1997; Duronio et al., 1998). More generally, we conclude that reducing rates of disc cell division does not immediately reduce rates of cell growth and so leads to increased cell size. However, cell cycle slowing or arrest does eventually suppress the accumulation of mass (see below, Johnston et al., 1977; Weigmann et al., 1997). We attribute this to the limiting amounts of DNA produced and also to the competitive disadvantage and poor viability of slowly dividing cells.

Disc Cell Size Varies According to Stage and Identity

To characterize the normal relationship of cell growth to cell cycle progression, we dissociated wild-type discs into single cells and used a fluorescence-activated cell sorter (FACS) to collect data for cell numbers, cellular DNA content, and forward light scatter (FSC), a measurement of cell size (Figure 2). Using precisely staged discs

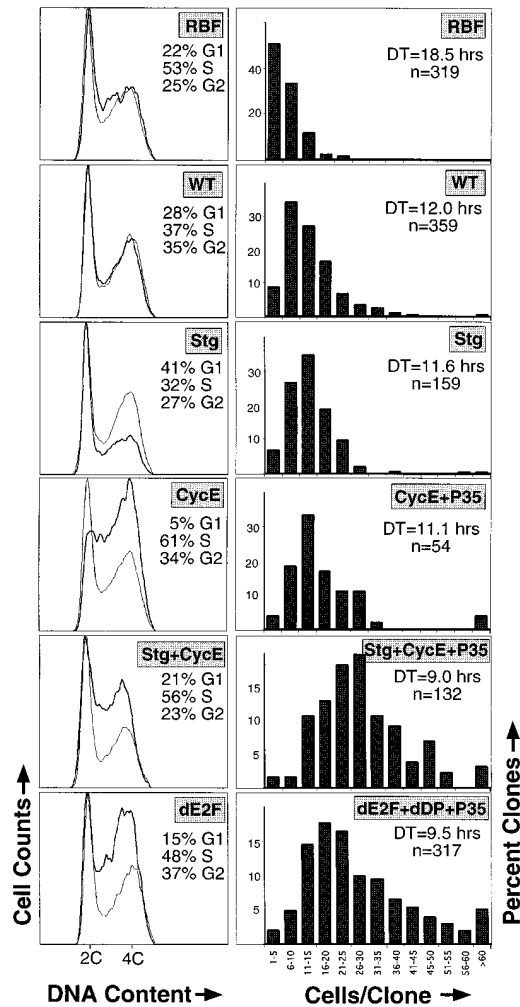


Figure 3. Analysis of Wing Disc Cell Cycle Regulation
 Left column, FACS analysis of wing disc cells at 94 ± 2 hr AED, showing altered cell cycle phasing. The indicated cell cycle regulators and GFP were expressed under en-GAL4 control in posterior compartments. Histograms display DNA content (x) and cell numbers (y). Thin lines indicate anterior control cells; thick lines indicate transgene-expressing cells. G1, S, and G2 percentages refer to transgene-expressing cells only.
 Right column, overexpressed cell cycle regulators alter cell doubling times. Clones of cells expressing the indicated cell cycle regulators and GFP under Act>GAL4 control were induced at 72 hr AED and fixed for analysis 43 hr later. Cells in each clone were counted. Median cell doubling times (DT) and number of clones scored (n) are indicated in each panel.

we confirmed previous reports that disc cells accumulate in G2 during late third instar, as the cell cycle begins to slow (Figure 2C; García-Bellido and Merriam, 1971; Fain and Stevens, 1982; Graves and Schubiger, 1982). As their cycle slows, disc cells also progressively decrease in size (Figure 2D; Madhavan and Schneiderman, 1977). To mark a specific subpopulation of cells, we used the *engrailed*-GAL4 (en-GAL4) transgene to activate expression of a UAS-GFP transgene in posterior wing compartments (Figure 2A; Brand and Perrimon, 1993). Since green fluorescent protein (GFP) is readily detected by FACS (Figure 2B), this allowed us to compare DNA contents and sizes of anterior (A) and posterior

(P) cells. At early time points P cells were larger than A cells, but they divided more rapidly than A cells (García-Bellido and Merriam, 1971; D. Prober and B. A. E, unpublished data) and eventually became smaller (Figure 2F). Interestingly, the proportions of G1, S, and G2 in A and P cell populations remained indistinguishable despite their differing cell sizes and division rates (Figures 2E and 3). This suggests that cell growth rates are integrated with division rates throughout the cycle, rather than at a single control point such as the G1/S transition. More generally, these observations show that rates of cell division and cell growth are only loosely coupled and vary independently according to developmental stage and the spatial position of cells within the disc.

Targeted Overexpression of Cell Cycle Regulators

We used two techniques to overexpress cell cycle regulators in the disc. The first technique employed the posterior-specific en-GAL4 “driver” to coactivate expression of UAS-linked cell cycle genes along with UAS-GFP. Since en-GAL4 expresses continuously from the earliest stages of disc formation until maturation of the wing, this allowed us to study the effects of changes in steady-state levels of target gene expression in a defined cell population over as many as ten cell cycles (Figure 3). Our second approach utilized the “flip-out” GAL4 driver (Act>GAL4) to coactivate permanent, heritable expression of UAS-linked targets in random clones of cells. This technique employs heat-shock induction of the FLP recombinase to fuse an Actin 5c promoter to GAL4, generating random clones of GAL4 expressing cells at a precisely defined time point (Pignoni and Zipursky, 1997). At set intervals after inducing HS-FLP, we counted the number of GFP-positive cells per clone (Figure 3) and measured the area of epithelium they occupied (Figure 7). This enabled us to determine *in vivo* rates of cell division and clonal growth (i.e., increases in area) for cells expressing UAS-driven transgenes.

Previous studies have shown that cell cycle deregulation in imaginal discs often induces cell death (Asano et al., 1996; Du et al., 1996a; Milán et al., 1997), and that this can be effectively blocked by baculovirus P35, a Caspase inhibitor (Hay et al., 1994). We reasoned that cell death could confound our attempts to measure cell cycle and growth rates, and so we coexpressed P35 along with UAS linked cell cycle regulators in many experiments. By itself P35 had no detectable effects on the cell cycle, growth, or developmental timing (data not shown). It did, however, block cell death caused by dE2F, RBF, CYCE, or STG+CYCE (Figures 4E and 4F).

Cyclin E Limits S-Phase Initiation, and String (Cdc25) Limits M-Phase Initiation

Using the FACS/GFP method, we found that constitutive, en-GAL4-driven expression of the mitotic inducer STG dramatically decreased the fraction of G2 cells (Figure 3). Constitutive expression of the S-phase initiator CYCE had the complementary effect: it virtually eliminated the G1 cell population (Figure 3). We know that both genes must be expressed every other cell cycle for continued cell proliferation (Figure 1A and data not shown) and that both genes are expressed in periodic

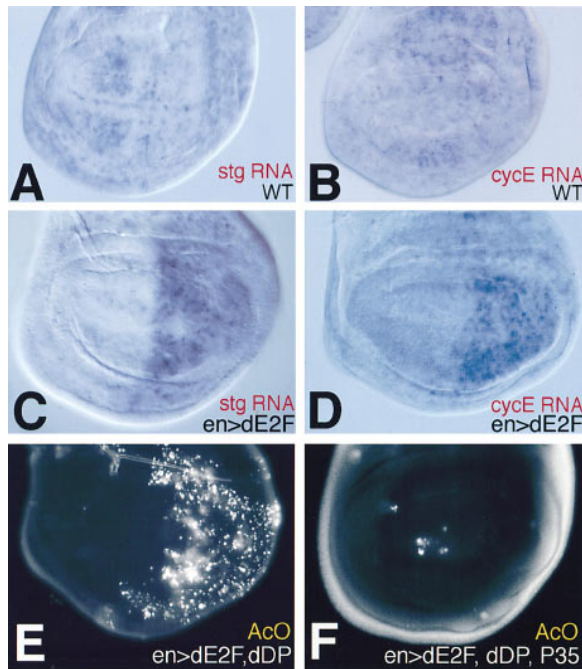


Figure 4. Effects of Ectopic dE2F

In situ hybridizations to RNA show the normal, dappled expression of *string* (A) and *cyclin E* (B) mRNAs in the wing pouch and the nearly ubiquitous induction of both *string* (C) and *cyclin E* (D) in posterior compartments overexpressing dE2F. (E) and (F) show discs stained with acridine orange (AcO) to detect cell death. Posterior expression of dE2F+dDP caused apoptosis (E), and coexpression of baculovirus P35 suppressed this apoptosis (F).

patterns (Figures 4A and 4B; Milán et al., 1996a). Therefore, we conclude that CYCE levels determine the length of G1 and that STG levels determine the length of G2.

To ask whether ectopic STG or CYCE affected rates of cell proliferation, we activated each gene clonally using the “flip-out” Act>GAL4 driver. Surprisingly, cells overexpressing either STG or CYCE had doubling times very similar to controls (STG = 11.6 hr, CYCE = 11.1 hr, WT = 12.0 hr; Figure 3). Using these cell doubling times and DNA profiles derived by FACS, we calculated the average duration of cell cycle phases. In WT cells G1 = 3.4 hr, S = 4.4 hr, and G2 = 4.2 hr. In CYCE overexpressing cells G1 = 0.6 hr, S = 6.8 hr, and G2 = 3.8 hr. In STG overexpressing cells G1 = 4.8 hr, S = 3.7 hr, and G2 = 3.1 hr. Apparently, cells overexpressing CYCE compensated for time lost in G1 by extending S phases, whereas cells overexpressing STG compensated for time lost in G2 by extending G1. Consistent with this, en-GAL4-driven expression of either STG or CYCE in posterior wing compartments did not alter the number of posterior cells significantly (Figure 6A).

dE2F Induces Both Cyclin E and String and Accelerates the Cell Cycle

In further tests, we found that induction of the dE2F transcription factor by Act>GAL4 driver shortened the average cell doubling time from 12 to 9.5 hr (Figure 3). In this accelerated cell cycle, both gap phases were abbreviated (G1 = 1.4 hr, S = 4.6 hr, G2 = 3.5 hr; Figure

3). Consistent with this observation, posterior expression of dE2F by en-GAL4 nearly doubled the number of posterior cells (Figure 6A). All of E2F’s effects were increased when it was coexpressed with dDP, an obligatory activating subunit (Figures 6A and 6C).

How does dE2F accelerate cell cycle progression? In situ hybridizations to RNA showed that ectopic dE2F induced strong, nearly ubiquitous expression of both *string* and *cyclin E* (Figures 4C and 4D). Although dE2F-dependent activation of *cyclin E* is well documented (Duronio et al., 1996; Rozyman et al., 1997), a role for dE2F in inducing the mitotic regulator *string* was unexpected. We considered the possibility that the induction of *string* resulted indirectly, from dE2F’s effects on cell cycle phasing or cell death. However, this proved unlikely since ectopic dE2F induced *string* mRNA in virtually all cells, apparently regardless of cell cycle phase (Figure 4C), and even after apoptosis was suppressed by the Caspase inhibitor P35 (data not shown).

To test whether simultaneous induction of CYCE and STG was the mechanism by which dE2F accelerated cell proliferation, we coexpressed both CYCE and STG under GAL4 control. We found that cells coexpressing CYCE+STG proliferated just as rapidly as dE2F overexpressing cells (doubling time = 9.0 hr). Moreover, these cells displayed a G1/S/G2 phasing much like dE2F overexpressing cells (G1 = 1.9 hr, S = 5.0 hr, G2 = 2.1 hr; Figure 3). Hence, we attribute the cell cycle acceleration caused by dE2F to its simultaneous induction of the G1/S regulator *cyclin E* and the G2/M regulator *string*.

RBF Slows Cell Cycle Progression

RBF, a *Drosophila* homolog of mammalian pRB, has been implicated as a dE2F antagonist by several criteria. RBF binds dE2F, it represses dE2F mediated transcriptional activation, and it suppresses morphological defects caused by dE2F overproduction in the fly eye (Du et al., 1996a). We found that clonal induction of RBF by Act>GAL4 increased the cell doubling time from 12.0 to 18.5 hr (Figure 3). FACS analysis of en-GAL4, UAS-RBF discs showed that RBF slowed all phases of cell cycle progression, with its greatest effect on S phase duration (G1 = 4.1 hr, S = 9.8 hr, G2 = 4.6 hr; Figure 3).

To test whether RBF’s effects were due to suppression of dE2F activity, we coexpressed RBF+dE2F using the en-GAL4 driver. Interestingly, RBF’s effects on cell cycle phasing, cell numbers, and cell size (see below) were dominant to, and augmented by, coexpressed dE2F (Figures 6A and 6C). This is consistent with the proposal of Weintraub et al. (1995), in which RB/E2F complexes actively repress transcription of E2F target genes. In situ hybridizations revealed that discs coexpressing RBF+dE2F had no ectopic induction of *string* or *cyclin E* transcripts (data not shown). Thus, RBF opposed the effects of dE2F on the transcriptional activation of target genes as well as on cell cycle progression.

In another test of RBF function, we coexpressed CYCE+STG+RBF using the en-GAL4 driver. FACS analysis and microscopic inspection of these discs showed that STG+CYCE bypassed the effects of RBF on cell size, cell numbers, and cell cycle phasing (Figures 6A and 6C). The dominance of STG+CYCE to RBF suggests that RBF probably exerts its effects upstream of *cyclin*

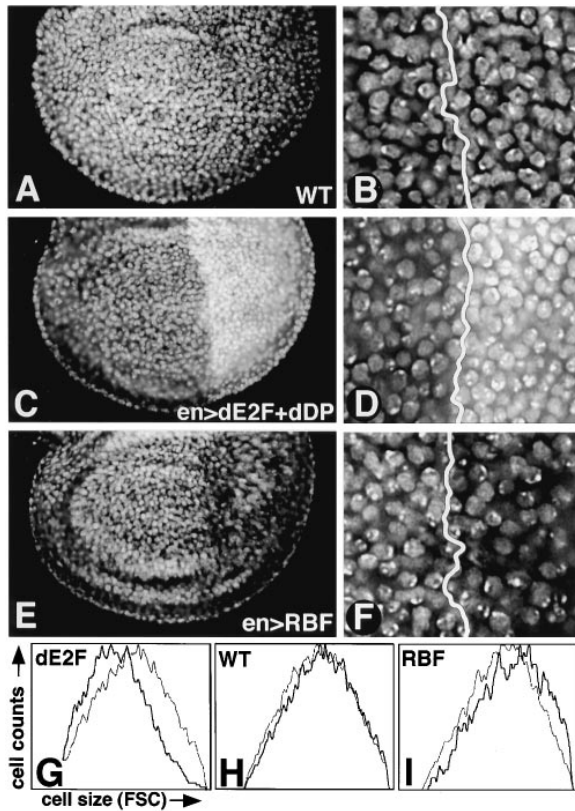


Figure 5. Ectopic Cell Cycle Gene Expression Alters Cell Size
 en-GAL4 was used to coexpress UAS-GFP and the UAS-transgenes noted, in posterior compartments. (A–F) Wing discs at ~100 hr AED stained for DNA to show differences in nuclear density. GFP is not shown, but the anterior-posterior compartment boundary is indicated by white lines in the high magnification panels (B, D, and F). Wild-type discs (A and B) show similar cell densities in both compartments, whereas overexpressed dE2F+dDP (C and D) increased posterior cell density, and RBF decreased it (E and F). Note that no alteration of posterior compartment size is evident. (G–I) show forward scatter (FSC) analysis of 94 ± 2 hr discs. Thin lines plot control, anterior cells, and thick lines plot experimental cells overexpressing dE2F (G), GFP only (H), or RBF (I).

E and *string* transcription. Therefore, these findings support the idea that overexpressed RBF slows the cell cycle by repressing the dE2F targets, *string* and *cyclin E*.

Compartment Growth Is Not Affected by Cell Cycle Deregulation

To determine whether these alterations in cell proliferation altered tissue growth, we measured the areas of anterior (A) and posterior (P) compartments in en-GAL4 discs at a series of developmental time points. Growth effects of GAL4 targets would be expected to change the ratio of P/A compartment size. Contrary to this, we found that changing the proliferative rate of P cells did not significantly affect the size of P compartments or their rates of growth relative to A compartments (Figures 5 and 6B). This remained true even when UAS-P35 was included to suppress cell death. In one exceptional case, larval development was extended for several days and posterior compartments did achieve larger than normal sizes (dE2F+dDP+P35; Figure 6B; see Discussion).

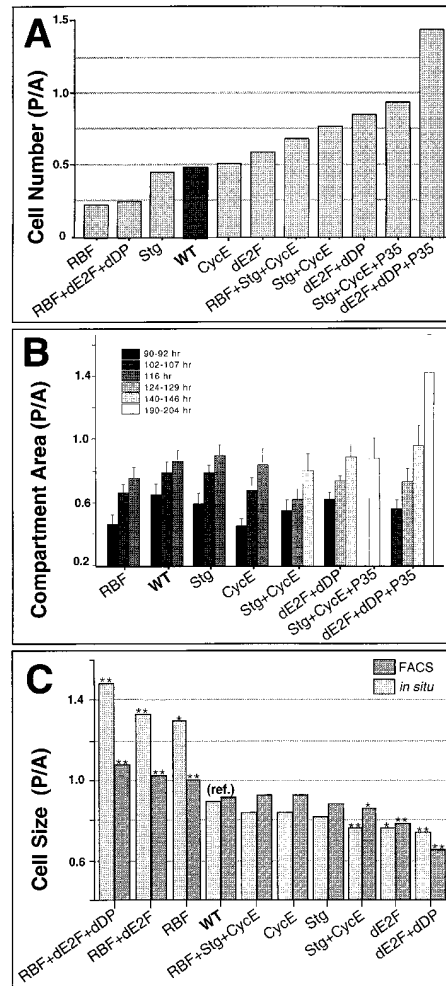


Figure 6. Cell Cycle Deregulation Alters Cell Numbers and Cell Size but Not Compartment Size

The indicated transgenes and GFP were expressed posteriorly using en-GAL4.

(A) Number of posterior (P) cells, plotted as ratios to number of anterior (A) cells. Data were summed from all FACS experiments (4–31 trials/genotype) giving $>10^5$ total cells for each genotype. Cell cycle retardation decreased P cell numbers, whereas cell cycle acceleration increased P cell numbers. Suppression of cell death by P35 further increased the cell number in these cases.

(B) P compartment areas plotted as ratios to A compartment areas at different developmental timepoints. Ten wing discs of each genotype were measured. P compartments are smaller than A compartments but grow faster. Ectopic expression of cell cycle regulators had insignificant effects on P compartment size, except in the case of dE2F+dDP+P35, which extended the larval phase and allowed growth beyond the normal size.

(C) Relative cell sizes, represented as P/A ratios. Cell size was determined by nuclear density determination of confocal sections of intact discs (in situ; light gray bars) or by forward scatter (FACS) measurement of cells from dissociated discs (FACS; dark gray bars). Transgene dependent decreases in cell size lower the P/A ratio, whereas increases in cell size increase this ratio. Each FACS experiment was repeated at least four times, and $>10^5$ cells were analyzed per experiment. For in situ data, four or more discs of each genotype were analyzed, and 280–511 nuclei were counted per section. P/A ratios represent median values. p values were calculated by the two-sample Wilcoxon rank-sum (Mann-Whitney) test, using WT as the reference group. Samples that were significantly different from WT are marked with asterisks (*, $p < 0.05$; **, $p < 0.01$).

However, even in this case the P compartment was normal in size throughout most of its development and grew at the normal rate.

As might be deduced from these results, altering the number of cells in the P compartment without changing its size resulted in striking changes in cell size. Cell size changes were readily visible (Figure 5) and were assessed by both FACS and cell density measurements made microscopically (Figure 6C). Both methods showed that accelerated proliferation correlated with decreased cell size, whereas retarded proliferation correlated with increased cell size. FACS data were analyzed to determine whether cell size changes were due to changes in cell cycle phasing, but in each case the experimental cells showed changes in average size during all cell cycle phases. Similar cell size effects were observed at all developmental stages tested, from early third instar (76 hr AED) to late pupation (160 hr AED; data not shown).

The observed relationship between cell numbers, compartment sizes, and cell sizes suggests that accumulation of mass in the P compartment progressed at the normal rate regardless of changes in cell division rates. Although it might be inferred that cell cycle deregulation has no effect on cell growth, there remained a further consideration. Studies of disc development have demonstrated that compartments function as units of size control (Garcia-Bellido et al., 1973; Simpson and Morata, 1981). Since expression of the en-GAL driver we used is itself compartmentally determined, we suspected that compartmental size controls might counteract any effects of GAL4 targets on growth.

Clonal Growth Is Regulated Independently of Cell Cycle Progression

To circumvent compartmental size controls, we used clonal gene activation. Mosaic analysis has shown that cell lineages *within* compartments are plastic and that clone sizes can be varied tremendously by varying cell growth capability (Garcia-Bellido et al., 1973; Simpson, 1979; Simpson and Morata, 1981). Hence, we assessed the size, in area, of clones expressing UAS-linked target genes under Act>GAL4 control (Figure 7). Forty-three hours after induction, clone areas for all genotypes tested were essentially unaffected by changes in proliferative rate. This remained true even when cell death was suppressed by coexpressed P35. For example, 43 hr RBF expressing clones had a median cell number of only 4, and CYCE+STG expressing clones of the same age had a median cell number of 24. Yet both clone types had similar median areas (554 and 619 μM^2 , respectively). As in the experiments using en-GAL4, the discrepancy between cell numbers and clonal areas could be explained by altered cell sizes, which were readily evident (Figure 7A).

As a more sensitive test, we induced Act>GAL4 clones very early in disc development (38 hr AED) and scored them 77 hr later (Figure 7B). A single clone with a growth advantage can take over as much as half the wing when induced this early (Simpson and Morata, 1981), whereas cells with a growth disadvantage are eliminated (Simpson, 1979; Table 1). We found that 77-hr-old clones expressing RBF+P35 were roughly half

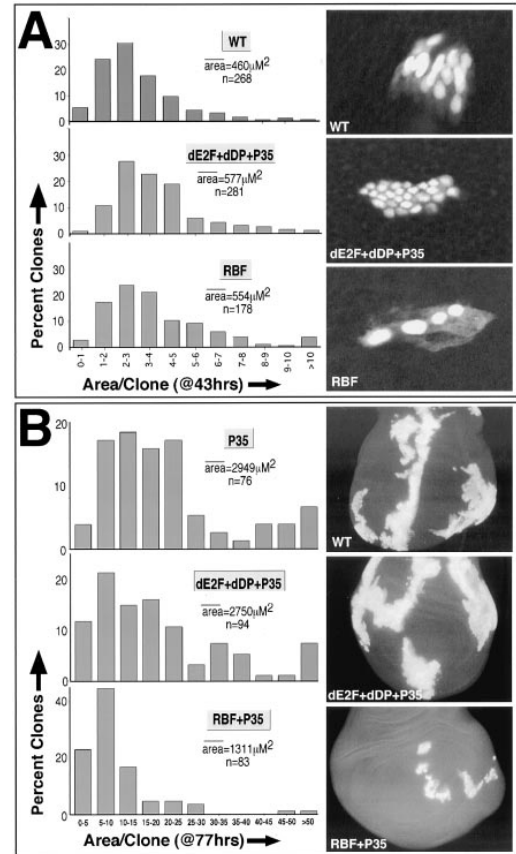


Figure 7. Cell Cycle Acceleration Does Not Increase Clonal Growth (A) Areas (left) and representative photos (right) of 43-hr-old clones expressing the indicated transgenes under Act>GAL4 control. Note the cell size changes at right, as visualized by the clonal marker, GFP-nls. Enlarged RBF expressing cells show large cytoplasmic extensions, whereas diminutive dE2F+dDP+P35 expressing cells have little visible cytoplasm. (B) Area measurements and representative photos of transgene expressing clones 77 hr after induction. Graphs show that ectopic dE2F+dDP+P35 confers no growth advantage, and they also reveal the eventual growth disadvantage imposed by ectopic RBF. Photos show entire wing anlage. Below each genotype we indicate median clone areas and numbers of clones measured (n). X axes have units of pixels $\times 10^{-3}$, where 1000 pixels = 169.4 μM^2 . Photos in (A) are the same magnification, as are those in (B).

the size of controls (1311 μM^2 vs. 2949 μM^2 ; n = 83, 76; Figure 7B). Thus, prolonged expression of RBF does eventually suppress growth. As in the case of *dE2F* loss, this probably reflects the limited amount of DNA produced by slowly cycling cells. Considering that RBF can act as a growth suppressor, the nearly normal size of posterior wing compartments expressing RBF (Figure 6) is probably due to the compensating effects of compartmental size control. In contrast, 77 hr clones of rapidly dividing cells expressing dE2F+dDP+P35 grew to sizes comparable to controls but no larger (Figure 7B). These clones had a median area of 2750 μM^2 (n = 94) and control clones expressing P35 alone had a median area of 2949 μM^2 (n = 76). This agrees with results obtained using the en-GAL4 driver and confirms that accelerating cell proliferation by increasing dE2F activity does not accelerate growth.

Discussion

Even in yeast, where cell proliferation would seem to be a simple cell-autonomous response to nutrients, it remains unclear how the cell cycle machinery is coupled to increases in cell mass. This problem is more formidable in animal tissues where cell–cell communication networks, rather than nutrition, regulate cell proliferation. Here, we address the relationship of growth and cell cycle control in vivo in the developing wing of *Drosophila*. This system allowed us to probe questions not accessible in single-celled systems that lack cell–cell communication or in early embryos where massive reserves of maternal cytoplasm bypass the necessity for growth control.

Cell Cycle Controls in the Wing

Through loss- and gain-of-function experiments, we identified *cyclin E* and the Cdc25 homolog *string* as limiting regulators of S- and M-phase initiation in developing wings. Ectopic CYCE truncated G1 and ectopic STG truncated G2, but in either case cells compensated by lengthening other cell cycle phases. Such compensation has also been noted in single-celled systems, but the mechanisms involved remain unknown. In contrast, we found that the transcriptional regulator dE2F had the capability to regulate overall rates of cell proliferation. By deleting *dE2F* or ectopically expressing it in combination with its coactivator dDP or its corepressor RBF, we subjected cells to what we presume were seven different levels of dE2F activity ($dE2F^{-1}/dE2F^{-2} < GAL4-dE2F+dDP+RBF < GAL4-dE2F+RBF < GAL4-RBF < WT < GAL4-dE2F < GAL4-dE2F+dDP$). This revealed a simple relationship in which more dE2F activity gave faster cell cycles and less activity gave slower cell cycles. This correlation is most clearly illustrated by the progressive alterations in cell numbers and cell size that resulted from changing cell cycle rates (Figure 6). Thus, dE2F appears to satisfy a critical criterion as a dosage-sensitive regulator of rates of cell cycle progression. Further experiments led us to ascribe this property of E2F to its ability to promote expression of both *cyclin E* and *string*. This effectively shortened both gap phases, bypassed the compensatory mechanisms noted above, and decreased overall cell doubling times. E2F's ability to activate genes used in DNA replication has been shown in many systems, but this is one of the first reports of E2F-dependent activation of a limiting mitotic regulator (Cdc25/STG).

Functions of dE2F and RBF

Is dE2F also a growth regulator? If it were, it might have behaved like the *Minutes*, which alter growth and cell proliferation coordinately without affecting cell size (Simpson, 1979; Simpson and Morata, 1981; Figure 1). We found a different relationship, however: dE2F altered rates of cell cycle progression much more than rates of mass accumulation (growth), and dramatic changes in cell sizes resulted. The only significant growth affect we observed was that loss of dE2F or overexpression of its corepressor, RBF, eventually suppressed growth in cell clones. This is probably an indirect consequence, since

slowing reduplication of the genome must eventually limit biosynthetic capability (Johnston et al., 1977; Weigmann et al., 1997). Although increasing dE2F activity accelerated the rate of cell proliferation by 25%, it had no measurable affect on rates of mass accumulation (Figure 7). Therefore, we conclude that dE2F acts primarily as a cell cycle regulator and has little direct role in stimulating growth. RBF can act as a growth suppressor, but it appears to execute this function via retarding cell cycle progression.

One apparent contradiction to this conclusion is our finding that compartments overexpressing dE2F, dDP, and the apoptosis suppressor P35 grew larger than normal (Figure 6B). For unknown reasons this combination of transgenes extended larval development for several days. During this period the overexpressing cells accumulated in multiple layers and abnormal folds. We also observed a P35-dependent, multiple layering of cells in clones expressing dE2F+dDP or STG+CYCE. Although P35 blocked apoptosis in these cells, it apparently did not block their delamination from the disc epithelium. Based on this we suggest that the overgrowth of dE2F+dDP+P35 expressing compartments arose from the structural disorganization that ensued when cells marked for death were excluded from the epithelium but failed to die. Disrupting the epithelial organization of the disc may disturb the cell–cell communication used in compartmental size control and so lead to overgrowth (see also Watson et al., 1994).

Coordinating Division Rates with Growth

A logical thesis posed by our findings is that disc cells could use growth-dependent modulation of dE2F activity to coordinate the accumulation of mass with rates of division. Evidence for this in the wing is compelling but not yet conclusive. dE2F is required for normal proliferation of wing cells, and alterations in dE2F activity can indeed change rates of cell division in a dose-dependent fashion. dE2F targets such as *cyclin E*, *string*, and *ribonucleotide reductase 2* are normally expressed in periodic patterns in the growing wing, and these patterns might reflect growth-dependent transcription. Moreover, cell sizes and division rates vary in different regions of the disc, yet the G1/S/G2 phasing of cells remains quite uniform (Figure 2). Since dE2F affects G1/S and G2/M progression coordinately, this is consistent with a scenario in which endogenous dE2F activity varies from cell to cell and is higher in more rapidly cycling cells.

Contrary to this thesis, dE2F is probably only one of many regulators of *cyclin E* and *string* in imaginal discs (Johnston and Edgar, 1998; Jones and Saint, unpublished data). Another consideration is that dE2F protein is normally expressed much more uniformly in the growing wing than its putative targets (our unpublished observations). This suggests that, as with the vertebrate E2Fs, regulation of *Drosophila* E2F is likely to occur through phosphorylation of cofactors like RBF rather than via modulated expression. Overexpressed dE2F presumably has activity because it exceeds the levels of endogenous posttranslational regulators like RBF, but this may not recapitulate the mechanisms actually

used *in vivo*. Further testing of the thesis that dE2F links growth rates to cell cycle progression will entail demonstrating that endogenous dE2F activity varies *in vivo* and deciphering whether and how such variation might be coupled to growth.

Despite these gaps in our understanding, recent studies in other systems already provide clues about how this coupling might work. Connections have been drawn from growth factor signaling through the RAS pathway to the FRAP/TOR kinase and finally to the translational regulators eIF4E and S6K (Barbet et al., 1996; Sonenberg, 1996). It has also been proposed that RAS stimulates cell proliferation by suppressing the activity of pRB (Aktas et al 1997; Leone et al., 1997; Peeper et al., 1997). Thus, it is tempting to suggest that extracellular signals stimulate translation, and a translationally sensitive regulator, such as a D-type Cyclin, responds by accumulating to levels sufficient to activate E2F and its targets (Rosenwald et al., 1995; Sherr, 1996). Such a mechanism would couple translation rates to E2F activity and thus presumably also couple increases in cell mass to cell cycle progression. This type of regulation has been demonstrated recently in *Saccharomyces cerevisiae*, where nutritional conditions influence levels of the G1 Cyclin CLN3 through translational control (Barbet et al., 1996; Polymenis and Schmidt, 1997). We find that Cyclin E can weakly stimulate expression of dE2F targets in the fly wing, but in contrast to dE2F, Cyclin E's biological effects seem confined to G1/S progression (Figure 3; our unpublished observations, see also Duronio and O'Farrell, 1995). Moreover, we have so far failed to uncover a role for *Drosophila* Cyclin D in dE2F control (S. Datar and B. A. E., unpublished data; Finley et al., 1996). Thus, it remains unclear how dE2F activity might be coupled to translation rates.

Other modes of growth control are also possible. For instance, cell growth and cell cycle progression might respond to the patterning signals that control wing development though parallel, yet independent pathways (Johnston and Edgar, 1998). This could explain why wing cells vary in size at different developmental stages and in different regions of the patterning field (Figure 2). The finding that manipulations of *Ras1* and *PI3K* gene activity change cell sizes in the wing may also be consistent with this possibility (Diaz-Benjumea and Hafen, 1994; Leever et al., 1996; Karim and Rubin, 1998). Nevertheless, the fact that mutations in the protein synthesis machinery (the *Minutes*) retard cell proliferation without changing cell size leads us to favor the model proposed for yeast two decades ago, in which growth is upstream of and dominant to cell cycle controls (Johnston et al., 1977).

Experimental Procedures

Fly Stocks

UAS-dE2F, UAS-STG, and UAS-GFPnls lines were generated by P element-mediated transformation. Several transgenic lines were gifts: UAS-CYCE from C. Lehner, UAS-RBF and UAS-dDP from N. Dyson, UAS-P35 from B. Hay, *en-GAL4* from A. Brand, and UAS-GFP^{S65T} from B. Dickson. *stg^{7B}*, *stg^{9A}* (Edgar and O'Farrell, 1989), *dE2F⁷²⁹* (Brook et al., 1996), *Act>CD2>GAL4* (Pignoni and Zipursky, 1997), and *M(3)95A^{lacZ}* (Andersson et al., 1994) have been described. Clonal analysis was performed as per Xu and Rubin (1993).

dE2F⁷²⁹ is a P[LacZ] insertion-mutation that is null for function. *dE2F⁷²⁹* has been reverted by P element excision, and the reverted chromosome complements the *FRT dE2F⁷²⁹ π-myc* chromosome used here (N. Dyson, personal communication). Cells homozygous for the *FRT stg^{7B} π-myc* chromosome arm used can be rescued for division in wing discs by several *stg⁺* transgenes. Thus, the *FRT dE2F⁷²⁹ π-myc* and *FRT stg^{7B} π-myc* chromosomes used are presumed free of confounding secondary mutations.

UAS Transgenes

A 4.4 kb *dE2F* cDNA from pBS-dE2F (Dymlacht et al., 1994) was ligated into the EcoRI site of pUAST (Brand and Perrimon, 1993) to generate UAS-dE2F. A 2.3 kb XhoI/XbaI fragment containing the *stg* cDNA was ligated into pUAST to generate UAS-STG. For UAS-GFPnls, oligonucleotides encoding the nuclear localization signal of SV40 large T antigen preceded by a consensus initiation codon were ligated into HindIII/EcoRI-digested pBluescript SKII, generating pBS-nls. A 720 bp EcoRI/BamHI fragment encoding the GFP^{S65T} derivative was ligated into pBS-nls to generate pBS-GFPnls, and finally the full GFPnls insert was transferred as a XhoI/XbaI fragment into pUAST.

Flow Cytometry

Staged larvae derived from 2–3 hr egg collections and raised at 23°C were dissected in PBS. Wing discs were washed twice in PBS and incubated with gentle agitation for 2–4 hr in 500 μl PBTH (4.5 mg/ml porcine trypsin-EDTA [Intergen], 0.5 μg/ml Hoechst 33342 in PBS). Dissociated cells lost the columnar morphology observed *in situ* and became spherical (Figure 2B). Twenty to forty discs were generally dissociated. We used a Becton Dickinson FACS Vantage, and data were analyzed using Cell Quest (Becton Dickinson) and Multicycle AV (Phoenix Flow Systems) software.

Proliferation and Growth Rate Measurements

GAL4-expressing clones were induced by the FRT “flip out” method (Struhl and Basler, 1993; Pignoni and Zipursky, 1997) in HS-FLP, *Act5c>CD2>GAL4*, UAS-GFPnls (± additional UAS lines) animals. Larvae were heat shocked either at 38 ± 2 hr AED for 1 hr at 37°C, or at 72 ± 1 hr AED for 30 min at 34°C. Dissected discs were fixed at 115 hr AED. GFP-positive cells per clone were counted on a Leitz DMRD epifluorescence microscope. Cell doubling times were derived using the formula $\log N / \log 2$ (hr), where N = median cell number/clone and hr = age of the clone. To measure clone and compartment sizes, >10 discs from precisely staged larvae were imaged on a BioRad MRC-600 confocal microscope, and areas of GFP-positive tissue were determined using the histogram function of Adobe Photoshop.

Histology

Discs were fixed in 6% paraformaldehyde in PBS for 40 min, washed in PBS + 0.1% Tween 20, and mounted in Fluoroguard (BioRad). Rhodamine-phalloidin (Molecular Probes) and Hoechst 33258 (Acros) were used to label cell outlines and nuclei. Clonal markers were detected using anti-myc (1:50) or anti-β-Gal (1:10000) 1° antibodies (Oncogene Science and Cappel), and preabsorbed FITC-conjugated 2° antibodies (1:600; Jackson). To identify apoptotic cells, unfixed discs were incubated for 10 min in Schneider's culture medium containing acridine orange (1.6 μM), and mounted in Schneider's medium. High magnification fluorescent images were collected on a Deltavision S/A30 microscope. *In situ* hybridizations were carried out using digoxigenin-labeled RNA probes as described (Tautz and Pfeifle, 1989).

Acknowledgments

We thank Nick Dyson and Christian Lehner for gifts of flies and reagents; Dara Lehman, Michele Garfinkel, and Bre Holt for their contributions to the early stages of this work; Kristy Seidel for expert help with statistics; and Nick Dyson, Lee Hartwell, Pat O'Farrell, Christian Lehner, and Jim Roberts for comments on the manuscript. Supported by National Institutes of Health GM51186 to B. A. E., American Chemical Society PF-4301 to T. N., and National Institutes

of Health GM17373 to L. A. J. Bruce Edgar is a Lucille P. Markey and Rita Allen Scholar.

Received January 8, 1998; revised May 15, 1998.

References

- Aktas, H., Cai, H., and Cooper, G.M. (1997). Ras links growth factor signaling to the cell cycle machinery via regulation of cyclin D1 and the Cdk inhibitor p27KIP1. *Mol. Cell. Biol.* **17**, 3850–3857.
- Andersson, S., Saeboe-Larsen, S., Lambertsson, A., Merriam, J., and Jacobs-Lorena, M. (1994). A *Drosophila* third chromosome Minute locus encodes a ribosomal protein. *Genetics* **137**, 513–520.
- Asano, M., Nevins, J.R., and Wharton, R.P. (1996). Ectopic E2F expression induces S-phase and apoptosis in *Drosophila* imaginal discs. *Genes Dev.* **10**, 1422–1432.
- Barbet, N.C., Schneider, U., Helliwell, S.B., Stansfield, I., Tuite, M.F., and Hall, M.N. (1996). TOR controls translation initiation and early G1 progression in yeast. *Mol. Biol. Cell* **7**, 25–42.
- Brand, A.H., and Perrimon, N. (1993). Targeted gene expression as a means of altering cell fates and generating dominant phenotypes. *Development* **118**, 401–415.
- Brook, A., Xie, J.-E., Du, W., and Dyson, N. (1996). Requirements for dE2F function in proliferating cells and in post-mitotic differentiating cells. *EMBO J.* **15**, 3676–3683.
- Bryant, P.J. (1996). Cell proliferation control in *Drosophila*: flies are not worms. *BioEssays* **18**, 781–784.
- Burke, R., and Basler, K. (1996). Dpp receptors are autonomously required for cell proliferation in the entire developing *Drosophila* wing. *Development* **122**, 2261–2269.
- Cavanaugh, A.H., Hempel, W.M., Taylor, L.J., Rogalsky, V., Todorov, G., and Rothblum, L.I. (1995). Activity of RNA polymerase I transcription factor UBF blocked by *Rb* gene product. *Nature* **374**, 177–180.
- Diaz-Benjumea, F.J., and Hafen, E. (1994). The sevenless signaling cassette mediates *Drosophila* EGF receptor function during epidermal development. *Development* **120**, 569–578.
- Doherty, D., Feger, G., Younger-Shepherd, S., Jan, L.Y., and Jan, Y.N. (1996). Delta is a ventral to dorsal signal complementary to Serrate, another Notch ligand, in *Drosophila* wing formation. *Genes Dev.* **10**, 421–434.
- Du, W., Vidal, M., Xie, J.-E., and Dyson, N. (1996a). *RBF*, a novel RB-related gene that regulates E2F activity and interacts with *cyclin E* in *Drosophila*. *Genes Dev.* **10**, 1206–1218.
- Du, W., Xie, J.E., and Dyson, N. (1996b). Ectopic expression of dE2F and dDP induces cell proliferation and death in the *Drosophila* eye. *EMBO J.* **15**, 3684–3692.
- Duronio, R.J., and O'Farrell, P.H. (1995). Developmental control of the G1 to S transition in *Drosophila*: cyclin E is a limiting downstream target of E2F. *Genes Dev.* **9**, 1456–1468.
- Duronio, R.J., Brook, A., Dyson, N., and O'Farrell, P.H. (1996). E2F-induced S phase requires *Cyclin E*. *Genes Dev.* **10**, 2505–2513.
- Duronio, R.J., Bonnette, P.C., and O'Farrell, P.H. (1998). Mutation of the *Drosophila* *dDP*, *dE2F*, and *cyclin E* genes reveal distinct roles for the E2F/DP transcription factor and cyclin E during the G1-S transition. *Mol. Cell. Biol.* **18**, 141–151.
- Dynlacht, B.D., Brook, A., Dembski, M., Yenush, L., and Dyson, N. (1994). DNA-binding and trans-activation properties of *Drosophila* E2F and DP proteins. *Proc. Natl. Acad. Sci. USA* **91**, 6359–6363.
- Edgar, B.A., and Lehner, C.F. (1996). Developmental control of cell cycle regulators: a fly's perspective. *Science* **274**, 1646–1652.
- Edgar, B.A., and O'Farrell, P.H. (1989). Genetic control of cell division patterns in the *Drosophila* embryo. *Cell* **57**, 177–187.
- Fain, M.J., and Stevens, B. (1982). Alterations in the cell cycle of *Drosophila* imaginal disc cells precede metamorphosis. *Dev. Biol.* **92**, 247–258.
- Fero, M.L., Rivkin, M., Tasch, M., Porter, P., Carow, C.E., Firpo, E., Perlmutter, R.M., Kaushansky, K., and Roberts, J.M. (1996). A syndrome of multiorgan hyperplasia with features of gigantism, tumorigenesis, and female sterility in p27^{Kip1}-deficient mice. *Cell* **85**, 733–744.
- Finley, R.L., Jr., Thomas, B.J., Zipursky, S.L., and Brent, R. (1996). Isolation of *Drosophila* Cyclin D, a protein expressed in the morphogenetic furrow before entry into S phase. *Proc. Natl. Acad. Sci. USA* **93**, 3011–3015.
- Franch, H.A., Shay, J.W., Alpern, R.J., and Preisig, P.A. (1995). Involvement of pRB family in TGFbeta-dependent epithelial cell hypertrophy. *J. Cell Biol.* **129**, 245–254.
- Garcia-Bellido, A., and Merriam, J.R. (1971). Parameters of the wing imaginal disc development in *Drosophila melanogaster*. *Dev. Biol.* **26**, 61–87.
- Garcia-Bellido, A., Ripoll, P., and Morata, G. (1973). Developmental compartmentalisation of the wing disk of *Drosophila*. *Nature New Biol.* **245**, 251–253.
- González-Gaitán, M., Capdevila, M.P., and Garcia-Bellido, A. (1994). Cell proliferation patterns in the wing imaginal disc of *Drosophila*. *Mech. Dev.* **40**, 183–200.
- Graves, B.J., and Schubiger, G. (1982). Cell cycle changes during growth and differentiation of imaginal leg discs in *Drosophila melanogaster*. *Dev. Biol.* **93**, 104–110.
- Hartwell, L.H. (1971). Genetic control of the cell division cycle in yeast: II. genes controlling DNA replication and its initiation. *J. Mol. Biol.* **59**, 183–194.
- Hay, B.A., Wolff, T., and Rubin, G.M. (1994). Expression of baculovirus P35 prevents cell death in *Drosophila*. *Development* **120**, 2121–2129.
- Hemerly, A., de Almeida Engler, J., Bergounioux, C., Van Montagu, M., Engler, G., Inzé, D., and Ferreira, P. (1995). Dominant negative mutants of the Cdc2 kinase uncouple cell division from iterative plant development. *EMBO J.* **14**, 3925–3936.
- Herrera, R.E., Sah, V.P., Williams, B.O., Mäkelä, T.P., Weinberg, R.A., and Jacks, T. (1996). Altered cell cycle kinetics, gene expression, and G1 restriction point regulation in *Rb*-deficient fibroblasts. *Mol. Cell. Biol.* **16**, 2402–2407.
- Johnson, D.G., Schwarz, J.K., Cress, W.D., and Nevins, J.R. (1993). Expression of transcription factor E2F1 induces quiescent cells to enter S phase. *Nature* **365**, 349–352.
- Johnston, L.A., and Edgar, B.A. (1998). Wingless and Notch regulate cell-cycle arrest in the developing *Drosophila* wing. *Nature*, in press.
- Johnston, G.C., Pringle, J.R., and Hartwell, L.H. (1977). Coordination of growth with cell division in the yeast *Saccharomyces cerevisiae*. *Exp. Cell Res.* **105**, 79–98.
- Karim, F.D., and Rubin, G.M. (1998). Ectopic expression of activated Ras1 induces hyperplastic growth and increased cell death in *Drosophila* imaginal tissues. *Development* **125**, 1–9.
- Kipreos, E.T., Lander, L.E., Wing, J.P., He, W.W., and Hedgecock, E.M. (1996). Cul-1 is required for cell-cycle exit in *C. elegans* and identifies a novel gene family. *Cell* **85**, 829–839.
- Lecuit, T., Brook, W.J., Ng, M., Calleja, M., Sun, H., and Cohen, S.M. (1996). Two distinct mechanisms for long-range patterning by Decapentaplegic in the *Drosophila* wing. *Nature* **381**, 387–393.
- Leevers, S.J., Weinkove, D., MacDougall, L.K., Hafen, E., and Waterfield, M.D. (1996). The *Drosophila* phosphoinositide 3-kinase Dp110 promotes cell growth. *EMBO J.* **15**, 6584–6594.
- Leone, G., DeGregori, J., Sears, R., Jakoi, L., and Nevins, J.R. (1997). Myc and Ras collaborate in inducing accumulation of active cyclin E/Cdk2 and E2F. *Nature* **387**, 422–426.
- Madhavan, M., and Schneiderman, H.A. (1977). Histological analysis of the dynamics of growth of imaginal discs and histoblast nests during the larval development of *Drosophila melanogaster*. *Wilhelm Roux's Arch.* **183**, 269–305.
- Milán, M., Campuzano, S., and Garcia-Bellido, A. (1996a). Cell cycling and patterned cell proliferation in the *Drosophila* wing during metamorphosis. *Proc. Natl. Acad. Sci. USA* **93**, 11687–11692.
- Milán, M., Campuzano, S., and Garcia-Bellido, A. (1996b). Cell cycling and patterned cell proliferation in the wing primordium of *Drosophila*. *Proc. Natl. Acad. Sci. USA* **93**, 640–645.

- Milán, M., Campuzano, S., and Garcia-Bellido, A. (1997). Developmental parameters of cell death in the wing disc of *Drosophila*. Proc. Natl. Acad. Sci. USA 94, 5691–5696.
- Mitchison, J.M. (1971). The biology of the cell cycle. (London: Cambridge University Press).
- Nurse, P., Thuriaux, P., and Nasmyth, K. (1976). Genetic control of the cell division cycle in the fission yeast *Schizosaccharomyces pombe*. Mol. Gen. Genet. 146, 167–178.
- Ohtani, K., and Nevins, J.R. (1994). Functional properties of a *Drosophila* homolog of the E2F1 gene. Mol. Cell. Biol. 14, 1603–1612.
- Ohtsubo, M., and Roberts, J.M. (1993). Cyclin-dependent regulation of G1 in mammalian fibroblasts. Science 259, 1908–1912.
- Peeper, D.S., Upton, T.M., Ladha, M.H., Neuman, E., Zalvide, J., Bernards, R., DeCaprio, J.A., and Ewen, M.E. (1997). Ras signaling linked to the cell-cycle machinery by the retinoblastoma protein. Nature 386, 177–181.
- Pignoni, F., and Zipursky, S. (1997). Induction of *Drosophila* eye development by decapentaplegic. Development 124, 271–278.
- Polymenis, M., and Schmidt, E.V. (1997). Coupling of cell division to cell growth by translational control of the G1 cyclin CLN3 in yeast. Genes Dev. 11, 2522–2531.
- Quelle, D.E., Ashmun, R.A., Shurtleff, S.A., Kato, J.-y., Bar-Sagi, D., Rousel, M.F., and Sherr, C.J. (1993). Overexpression of mouse D-type cyclins accelerates G1 phase in rodent fibroblasts. Genes Dev. 7, 1559–1571.
- Reznitsky, D., Gossen, M., Bujard, H., and Reed, S.I. (1994). Acceleration of the G1/S phase transition by expression of cyclins D1 and E with an inducible system. Mol. Cell. Biol. 14, 1669–1679.
- Rosenwald, I.B., Kaspar, R., Rousseau, D., Gehrke, L., Leboulch, P., Chen, J.-J., Schmidt, E.V., Sonenberg, N., and London, I.M. (1995). Eukaryotic translation initiation factor 4E regulates expression of cyclin D1 at transcriptional and post-transcriptional levels. J. Biol. Chem. 270, 21176–21180.
- Royzman, I., Whittaker, A.J., and Orr-Weaver, T.L. (1997). Mutations in *Drosophila* DP and E2F distinguish G1-S progression from an associated transcriptional program. Genes Dev. 11, 1999–2011.
- Schnepf, B., Grumblin, G., Donaldson, T., and Simcox, A. (1996). Vein is a novel component in the *Drosophila* epidermal growth factor receptor pathway with similarity to the neuregulins. Genes Dev. 10, 2302–2313.
- Serrano, N., and O'Farrell, P.H. (1997). Limb morphogenesis: connections between patterning and growth. Curr. Biol. 7, R186–R195.
- Sheikh, M.S., Rochefort, H., and Garcia, M. (1995). Overexpression of p21WAF1/CIP1 induces growth arrest, giant cell formation and apoptosis in human breast carcinoma cell lines. Oncogene 11, 1899–1905.
- Sherr, C.J. (1996). Cancer cell cycles. Science 274, 1672–1677.
- Simpson, P. (1979). Parameters of cell competition in the compartments of the wing disc of *Drosophila*. Dev. Biol. 69, 182–193.
- Simpson, P., and Morata, G. (1981). Differential mitotic rates and patterns of growth in compartments in the *Drosophila* wing. Dev. Biol. 85, 299–308.
- Sonenberg, N. (1996). Translational control. In Translational Control, J.W.B. Hershey, M.B. Mathews, and N. Sonenberg, eds. (Cold Spring Harbor: Cold Spring Harbor Press), pp. 245–269.
- Struhl, G., and Basler, K. (1993). Organizing activity of wingless protein in *Drosophila*. Cell 72, 527–540.
- Tautz, D., and Pfeifle, C. (1989). A non-radioactive in situ hybridization method for the localization of specific RNAs in *Drosophila* embryos reveals translational control of the segmentation gene hunchback. Chromosoma 98, 81–85.
- Watson, K.L., Justice, R.W., and Bryant, P.J. (1994). *Drosophila* in cancer research: the first fifty tumor suppressor genes. J. Cell Sci. 108, 19–33.
- Weigmann, K., Cohen, S.M., and Lehner, C.F. (1997). Cell cycle progression, growth and patterning in imaginal discs despite inhibition of cell division after inactivation of *Drosophila* Cdc2 kinase. Development 124, 3555–3563.
- Weintraub, S.J., Chow, K.N.B., Luo, R.X., Zhang, S.H., He, S., and Dean, D.C. (1995). Mechanism of active transcriptional repression by the retinoblastoma protein. Nature 375, 812–815.
- White, R.J., Trouche, D., Martin, K., Jackson, S.P., and Kouzarides, T. (1996). Repression of RNA polymerase III transcription by the retinoblastoma protein. Nature 382, 88–90.
- Xu, T., and Rubin, G.M. (1993). Analysis of genetic mosaics in developing and adult *Drosophila* tissues. Development 117, 1223–1237.
- Zecca, M., Basler, K., and Struhl, G. (1995). Sequential organizing activities of engrailed, hedgehog and decapentaplegic in the *Drosophila* wing. Development 121, 2265–2278.